NASA/TM-20220002202

Natural Gas/Oxygen Burner Rig at The NASA Glenn Materials Research Laboratory

Dennis S. Fox, Michael J. Presby, Thomas M. Tomsik, Stephen L. McHargue, David. G. Meigs, Matthew. J. Shelton, Robert A. Miller, and Maria A. Kuczmarski
Glenn Research Center, Cleveland, Ohio

Michael D. Cuy
HX5, LLC, Brook Park, Ohio

March 2022

NASA STI Program . . . in Profile

Since its founding, NASA has been dedicated to the advancement of aeronautics and space science. The NASA Scientific and Technical Information (STI) Program plays a key part in helping NASA maintain this important role.

The NASA STI Program operates under the auspices of the Agency Chief Information Officer. It collects, organizes, provides for archiving, and disseminates NASA's STI. The NASA STI Program provides access to the NASA Technical Report Server—Registered (NTRS Reg) and NASA Technical Report Server—Public (NTRS) thus providing one of the largest collections of aeronautical and space science STI in the world. Results are published in both non-NASA channels and by NASA in the NASA STI Report Series, which includes the following report types:

- TECHNICAL PUBLICATION. Reports of completed research or a major significant phase of research that present the results of NASA programs and include extensive data or theoretical analysis. Includes compilations of significant scientific and technical data and information deemed to be of continuing reference value. NASA counter-part of peer-reviewed formal professional papers, but has less stringent limitations on manuscript length and extent of graphic presentations.

- TECHNICAL MEMORANDUM. Scientific and technical findings that are preliminary or of specialized interest, e.g., "quick-release" reports, working papers, and bibliographies that contain minimal annotation. Does not contain extensive analysis.

- CONTRACTOR REPORT. Scientific and technical findings by NASA-sponsored contractors and grantees.

- CONFERENCE PUBLICATION. Collected papers from scientific and technical conferences, symposia, seminars, or other meetings sponsored or co-sponsored by NASA.

- SPECIAL PUBLICATION. Scientific, technical, or historical information from NASA programs, projects, and missions, often concerned with subjects having substantial public interest.

- TECHNICAL TRANSLATION. English-language translations of foreign scientific and technical material pertinent to NASA's mission.

For more information about the NASA STI program, see the following:

- Access the NASA STI program home page at http://www.sti.nasa.gov

- E-mail your question to help@sti.nasa.gov

- Fax your question to the NASA STI Information Desk at 757-864-6500

- Telephone the NASA STI Information Desk at 757-864-9658

- Write to:
  NASA STI Program
  Mail Stop 148
  NASA Langley Research Center
  Hampton, VA 23681-2199

NASA/TM-20220002202

Natural Gas/Oxygen Burner Rig at The NASA Glenn Materials Research Laboratory

Dennis S. Fox, Michael J. Presby, Thomas M. Tomsik, Stephen L. McHargue, David. G. Meigs, Matthew. J. Shelton, Robert A. Miller, and Maria A. Kuczmarski
Glenn Research Center, Cleveland, Ohio

Michael D. Cuy
HX5, LLC, Brook Park, Ohio

National Aeronautics and
Space Administration

Glenn Research Center
Cleveland, Ohio 44135

March 2022

This work was sponsored by the
Transformative Aeronautics Concepts Program.

Level of Review: This material has been technically reviewed by technical management.

This report is available in electronic form at http://www.sti.nasa.gov/ and http://ntrs.nasa.gov/

Natural Gas/Oxygen Burner Rig at The NASA Glenn Materials Research Laboratory

Dennis S. Fox, Michael J. Presby, Thomas M. Tomsik,* Stephen L. McHargue, David. G. Meigs, Matthew. J. Shelton, Robert A. Miller,† and Maria A. Kuczmarski
National Aeronautics and Space Administration
Glenn Research Center
Cleveland, Ohio 44135

Michael D. Cuy
HX5, LLC
Brook Park, Ohio 44142

Abstract

This technical memorandum describes the development of a new natural gas/oxygen (NG/O_2) fueled burner rig to be used for high-temperature environmental durability studies of advanced materials and components at atmospheric pressure. The burner simulates the high-temperature, high-heat flux, and high-velocity thermal environments encountered in aerospace applications. It will be used to study environmental effects such as water vapor interactions relevant to advanced gas turbine engine materials such as ceramic matrix composites with protective environmental barrier coatings. The highest sample temperature achieved to date in a study of the oxidation and recession of monolithic silicon carbide is 3000 °F.

1.0 Introduction

The state-of-the-art Burner Rig Facility is located within the Materials Research Laboratory at the National Aeronautics and Space Administration's Glenn Research Center at Lewis Field (Ref. 1). It is used for materials research including oxidation, corrosion, erosion and impact. Within the facility are six identical Mach 0.3 computer-controlled jet-fueled combustors in individual test cells. In 2019 it was determined to add another type of burner rig. This new burner rig is a high-heat flux, natural gas/oxygen (NG/O_2) fueled combustion rig used for high-temperature environmental durability studies of advanced materials and components at atmospheric pressure. The burner simulates the high-temperature, high-heat flux, and high-velocity thermal environments encountered in aerospace engines and hypersonic vehicle leading edges. It will also be used to study environmental effects such as water vapor and contaminants relevant to advanced gas turbine engines. The rig bridges the gap between other laboratory methods such as jet-fueled burner rigs, lasers and expensive arc jet/rocket testing. The maximum sample temperature achieved with the M0.3 jet fueled rigs is ~2500 °F versus the 3000 °F achieved to date with the NG/O_2 rig. Another difference is the combustion of the natural gas/oxygen results in ~40 percent water vapor, versus ~10 percent for combustion of jet fuel. Accessibility and quick turnaround are added unique capabilities. The primary focus of this technical memorandum is to present an overview of the new burner rig and discuss its capabilities and use to date. This facility is primarily used for testing of advanced materials being developed under NASA Aeronautics Research Mission programs.

*Retired.
†Retired.

2.0 Description and Operation of the Natural Gas Burner Rig

Carlisle Machine Works (Millville, NJ) provides equipment for burner and combustion applications pertaining to the flame treatment of plastics and glass (Ref. 2). The unit herein is custom made and can consume up to 700 SCF/H of natural gas and 1500 SCF/H of oxygen (Figure 1). An interchangeable selection of their series 702, 705 or 707 lathe mount style surface mixed torches can be used. In the initial design the use of three torches at once was contemplated. However, computational fluid dynamics modelling revealed that the three flames would not combine to a single powerful jet. It became apparent that it was much better to force maximum flow through a single torch. The series 702 with 3/4 in. diameter gas ports is currently installed and mounted horizontally. The required hoses, solenoid valves, gas regulators, ignition/combustion controls, ball valves, mass flow controllers, check valves and E-stops are mounted within the power station platform.

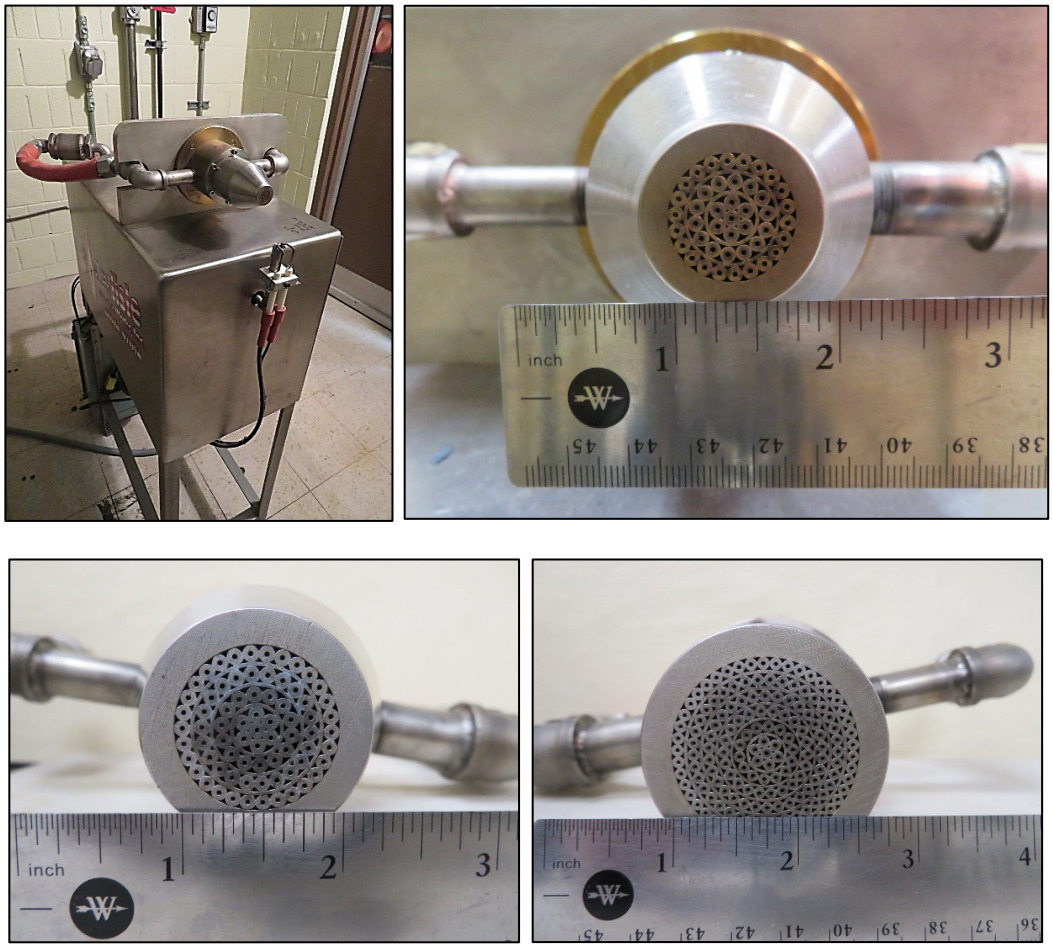

Figure 1.—Top left: Natural gas/oxygen burner and its platform. Top right: Currently installed series 702 burner nozzle with 3/4 in. diameter port. Bottom: Series 705 (1 in. diameter port) or 707 (1.5 in. diameter port).

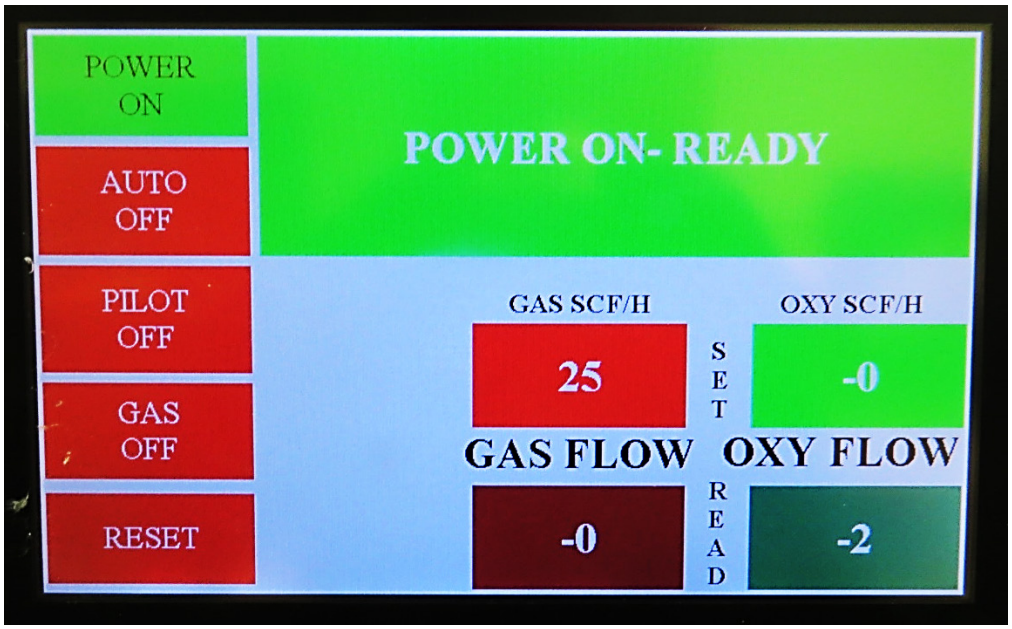

Figure 2.—Burner programmable logic controller (PLC) touchscreen.

The pilot burner has a dual electrode to ignite and sense the flame. The sensor is integrated with the O_2 and NG solenoid valves and an audible alarm. If no flame is detected, the system will shut down the gas flows and alert the operator. A programmable logic controller (PLC) with touchscreen (Allen Bradley) provides ignition, flame out alert, safety shutdown and expandable processing control (Figure 2).

The combustion fuel for the burner is natural gas from the building supply. The oxygen is supplied using an on-site oxygen generator system (Oxygen Generating Systems Intl., North Tonawanda, NY) in a room adjacent to the test cell. Per Figure 3, filtered 110 psig shop air from the building supply passes through a refrigerated air dryer (DRD250-230360, Parker Hannifin DRD250, Lancaster, NY) to remove water vapor (Ref. 3). A 120-gallon capacity service air receiving tank holds the dried air, which is then fed to a bank of three OG-500 oxygen generators (Ref. 4). The oxygen is separated from the air using OGSI's Pressure Swing Adsorption (PSA) Technology. The process centers around molecular sieve Zeolite (Ref. 5). Air contains roughly 78 percent nitrogen, 21 percent oxygen, 0.9 percent argon with the balance consisting of other gases. At high pressures the sieve adsorbs nitrogen, and at low pressures it desorbs (releases) nitrogen. Each OG-500 generator consists of two tanks filled with sieve. As high-pressure air (~70 psi) is introduced into the first tank, it passes through the sieve and nitrogen is adsorbed. The remaining oxygen and argon are piped to a buffer or storage tank. Just before the first tank becomes completely saturated with nitrogen, feed air is redirected to the second tank which then repeats the above process. The first tank is then vented to atmosphere which allows the nitrogen to desorb or release from the sieve. To complete the regeneration of the first tank, a small amount of the oxygen is used to purge it. This process is completed over and over again until the demand for oxygen is met. Under normal operating conditions, which includes our use of clean dry air for separation, the sieve will last indefinitely. Productivity of the PSA generator is dependent on the oxygen purity required. The oxygen generators used herein currently supply oxygen at ~93 percent purity as measured with a zirconia oxygen sensor (OC-40, Rotronic Measurement Solutions, Hauppauge NY). The 93 percent oxygen is stored in two 400-gallon capacity holding tanks (Figure 4).

Figure 3.—Left: Refrigerated air dryer and the service air receiving tank holding the dried air. Right: Bank of three OG-500 oxygen generators.

Figure 4.—Left to right: The service air receiving tank and two 93 percent oxygen storage tanks.

The burner was supplied with an Allen-Bradley® programmable logic controller (PLC). The automation software platform Wonderware was used to merge the Allen-Bradley® PLC and a Modicon PLC. One common program was developed for a Human Machine Interface (HMI) screen and historical data logging.

The Natural Gas/Oxygen Burner System Control Console (Figure 5) is the central location from where the entire rig can be controlled. It consists of a data acquisition computer for recording historical data on sample temperature, gas pressure, gas flow or any other telemetry sensors to be used when analyzing experiments. It also consists of a two-position key switch which allows the user the ability to remove and lock out power to the control console. The “system on” and E-stop buttons on the console allow a fast way to remove power in case of an emergency. When there is an alarm with the system, a light will blink, and an audible alarm will sound; both can be shut off with the horn reset button. The rig controller was shown and discussed per Figure 2. Finally, there is a touch screen control console Human Machine Interface (HMI) that communicates with the facility Modicon PLC that controls the supply of oxygen and natural gas to the burner.

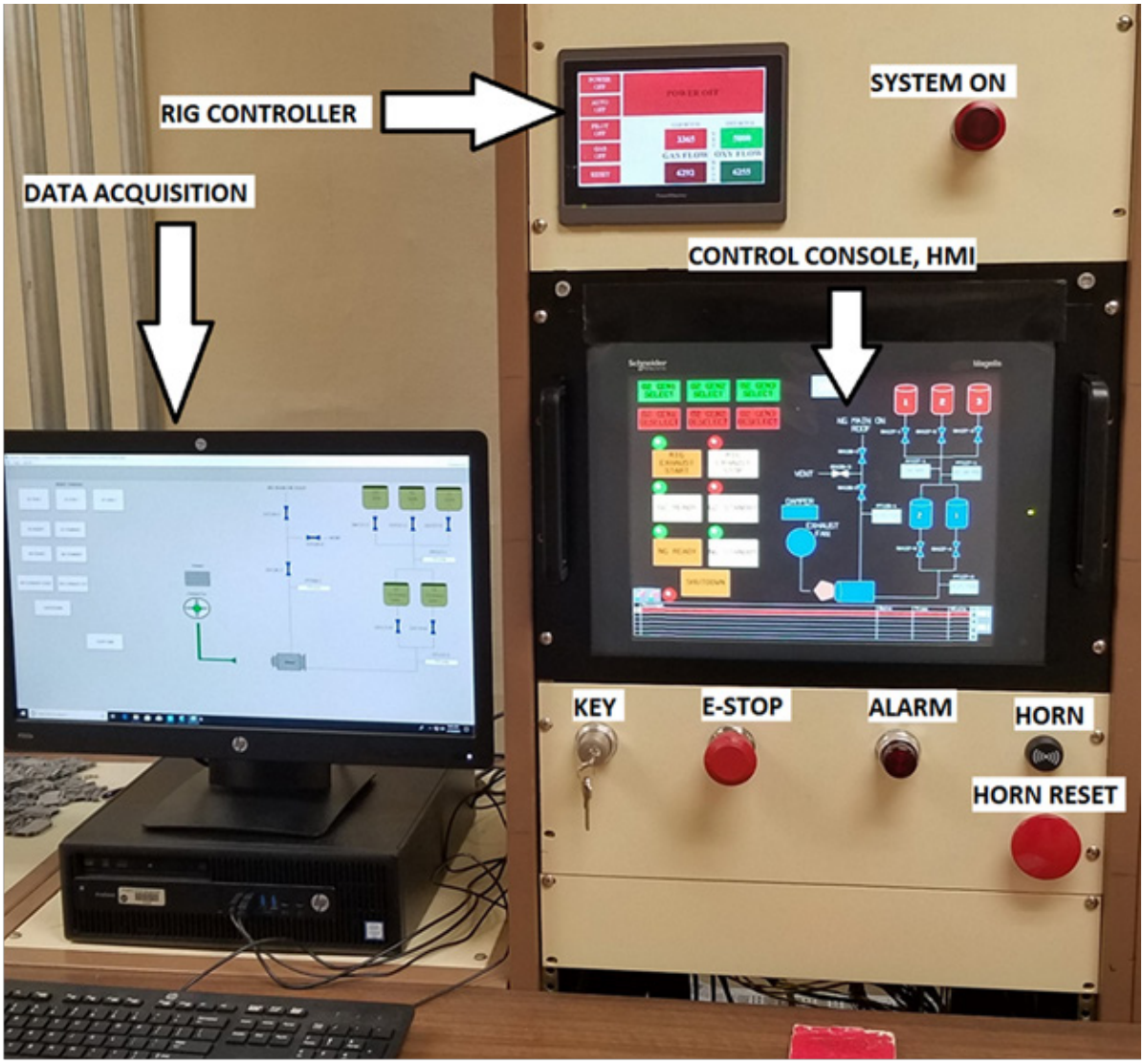

Figure 5.—Natural Gas/Oxygen Burner System Control Console.

The Natural Gas/Oxygen generation system Human Machine Interface (Figure 6) consists of three parts. The right side contains the Process and Instrumentation Diagram (P&ID). It is a visual reference of the system and its current state. Oxygen generators change color when selected, live pressure values are displayed, and valves change color to show if they are open (white) or closed (blue). The left side of the screen is the system controls which consists of oxygen generator selection and preparing the system for use of the natural gas and oxygen. The final part includes alarms and alerts for the whole system. Alert messages are to make the operator aware of a certain condition in the system. The alert does not mean immediate action is needed, but if the condition goes unchecked it could prevent the system from operating. An alarm message indicates an immediate condition has happened in the system. Most alarm messages have an automatic action performed in the system PLC which usually results in a forced shutdown of the system. Figure 7 shows the NG/O_2 rig during its initial operation.

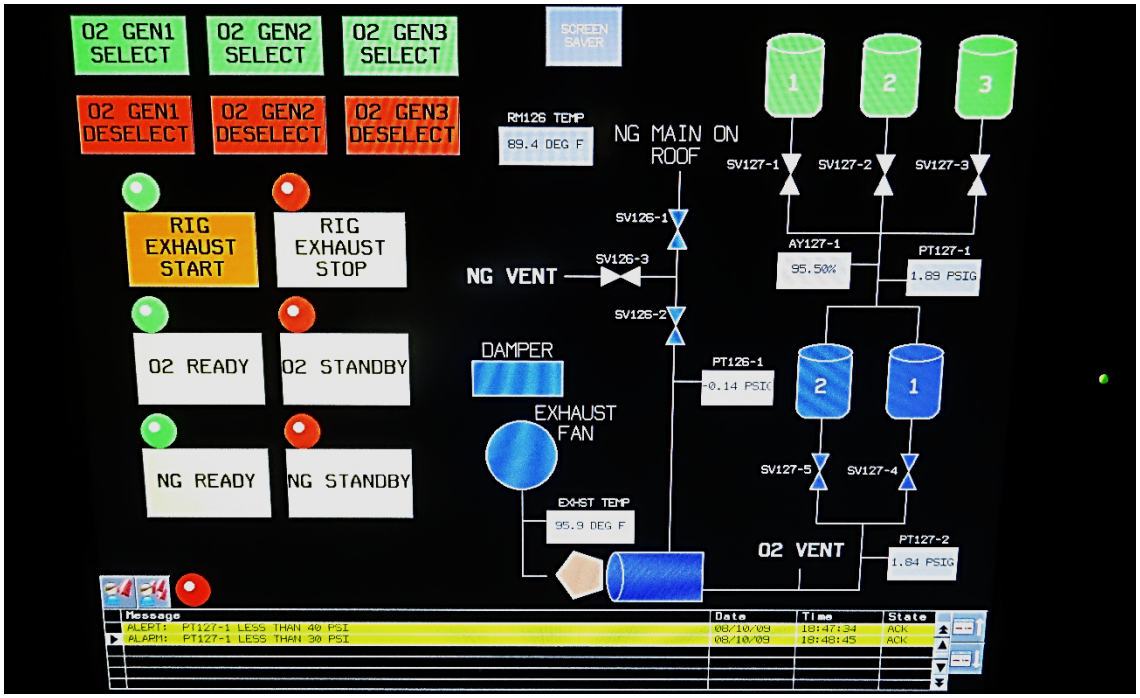

Figure 6.—Natural Gas/Oxygen generation system Human Machine Interface (HMI).

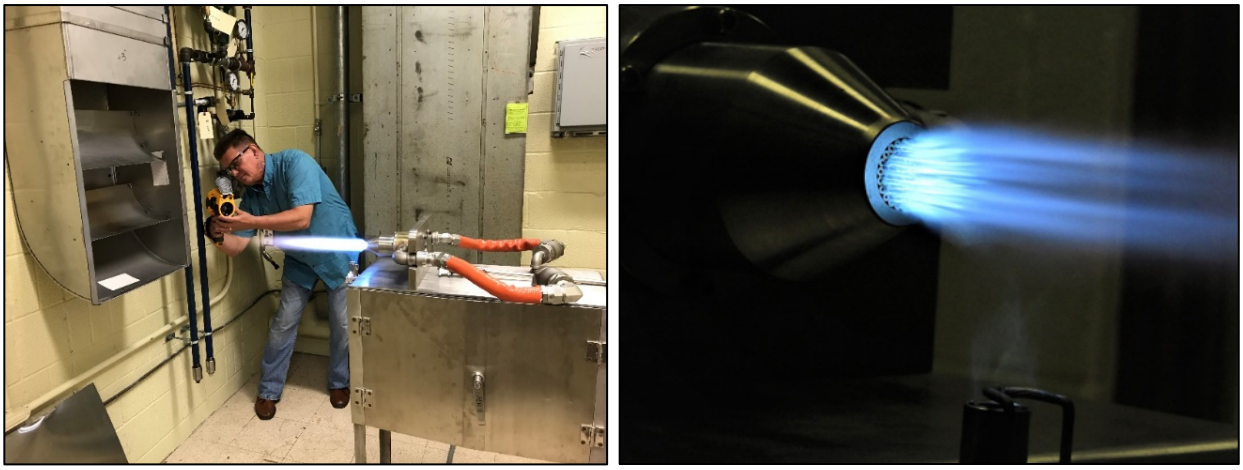

Figure 7.—NG/O_2 rig during its initial operation. Note the exhaust duct at the left. The piping system behind the engineer is for future backside cooling with shop air—either at room temperature or heated.

3.0 Combustion Analysis

The NASA Glenn Environmental Effects and Coatings Branch operates the natural gas burner rig. It requested combustion analysis from the Fluid and Cryogenic Systems Branch for an analysis to estimate flame temperatures over a range of equivalence ratios (Φ), operational fuel-to-air mixture ratios, and heat fluxes that might be achievable with the new burner. The scope of the analysis included:

(1) Estimate the key combustion properties of the natural gas fuel when reacted with oxygen enriched air at 93 percent O_2 and 7 percent N_2 by volume.
(2) Estimate possible air-to-fuel mixture ratios, equivalence ratios and combustion properties at stoichiometric conditions.
(3) Calculate the Adiabatic Flame Temperature (AFT) over a range of equivalence ratios with data curves.
(4) Estimate the Expected Flame Temperature (EFT) over a range of equivalence ratios with data curves.

    Note that the EFT is less than AFT due to heat losses and affects causing combustion inefficiency (i.e., incomplete combustion, dissociation, dilutants entering flame, imperfect mixing, etc.)

(5) Estimate the heat flux generated by the burner's flame impinging on a planar surface.

The composition of natural gas varies widely depending on supplier and location. The values in Table I were determined to be a reasonable approximation to the range of values found in the Ohio production region (Ref. 6).

The equivalence ratio (Φ) is commonly used in combustion calculations, where F/A is the fuel-to-air weight ratio. It is defined as:

$$\Phi = (F/A) / \text{Stoichiometric } (F/A)$$

Stoichiometric combustion is a theoretical position in which the optimal amount of oxygen and fuel generates the most heat possible, and maximum combustion efficiency is achieved. There are no unburned combustibles and no excess air. Similarly, the air-to-fuel weight ratio Θ is given by the mass of air (A) divided by the mass of fuel (F).

Equivalence ratios greater than one mean there is more fuel in the fuel–oxidizer mixture than required for complete combustion; this mixture is termed "rich." Equivalence ratios less than one means there is excess air or oxidizer in the combustion mixture. This mixture is termed "lean." An equivalence ratio equal to one means the combustion reaction is stoichiometric—a theoretical position in which the optimal amount of oxygen and fuel generates the most heat possible, and maximum combustion efficiency is achieved. There are no unburned combustibles and no excess oxygen.

TABLE I.—NATURAL GAS COMPOSITION USED IN ANALYSIS

Fuel gas component	Formula	Volume percent	Weight percent
Methane	CH_4	93.4	87.4
Ethane	C_2H_6	2.7	4.7
Propane	C_3H_8	0.6	1.5
Butane	C_4H_{10}	0.2	0.7
Carbon Dioxide	CO_2	0.7	1.8
Nitrogen	N_2	2.4	3.9
Total	------	100.0	100.0

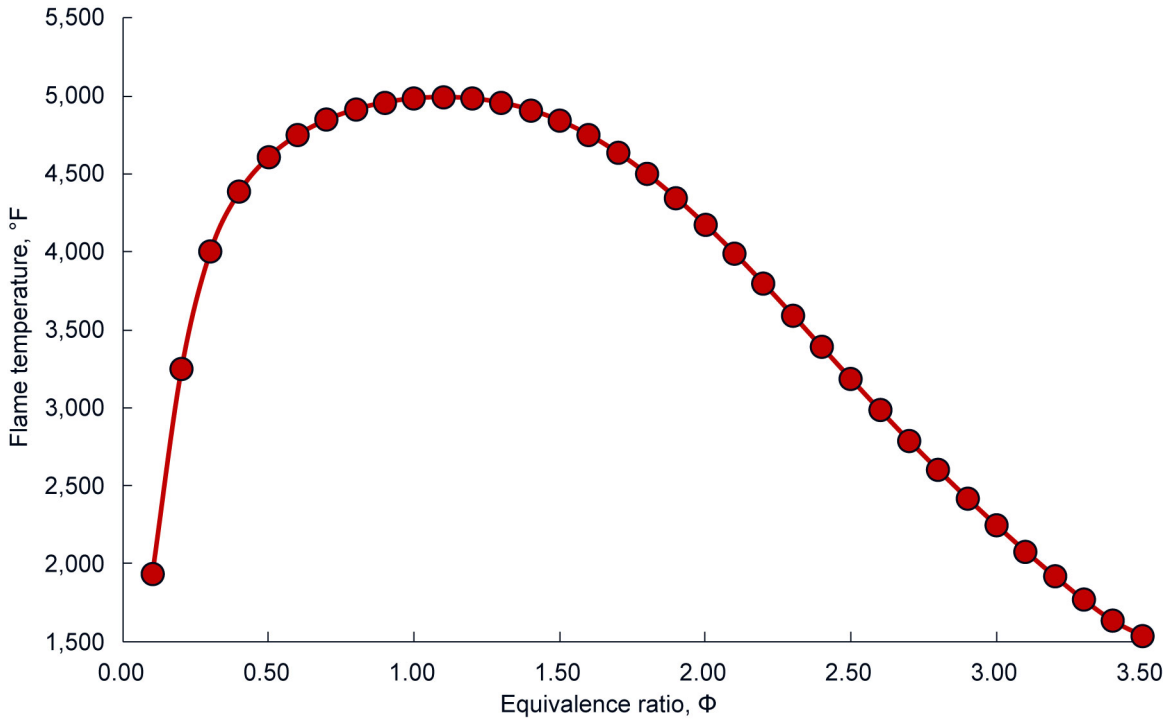

Figure 8.—Adiabatic Flame Temperature (AFT) vs. Equivalence Ratio, Φ, calculated with CEA program for Natural Gas with 93 percent Oxygen (O_2) and 7 percent Nitrogen (N_2).

The Adiabatic Flame Temperature (Figure 8) was calculated using the NASA Computer program CEA (Chemical Equilibrium with Applications) with both fuel and air at 77 °F and 14.7 psia. The program (https://cearun.grc.nasa.gov/) calculates chemical equilibrium compositions and properties of complex mixtures. Applications include assigned thermodynamic states, theoretical rocket performance, Chapman-Jouguet detonations, and shock-tube parameters for incident and reflected shocks. Associated with the program are independent databases with transport and thermodynamic properties of individual species. Over 2000 species are contained in the thermodynamic database. The program is written in ANSI standard FORTRAN by Bonnie J. McBride and Sanford Gordon (Ref. 7). It is in wide use by the aerodynamics and thermodynamics community, with over 2000 copies in distribution

The expected—or actual—flame temperature (EFT; Figure 9) will be cooler than the AFT, because heat transfer occurs from the flame to the surroundings via radiation, convection, and conduction heat losses. Air diluents can also enter the flame zone, slightly quenching the flame and causing the actual temperature to be less than theoretical calculated by CEA. EFT was calculated based on an energy balance around the flame using radiation dominating the total heat loss. Both fuel and air were at 77 °F and 14.7 psia.

A comparison of Adiabatic Flame Temperature to Expected Flame Temperature as a function of equivalence ratio (Φ) calculated with the CEA program is shown in Figure 10. Table II summarizes the results of the combustion analysis. It should be noted that the values in Table II are estimates from the combustion analysis, and further validation and rig characterization is required. For example, lower or higher sample temperatures may be achievable depending upon sample properties, stand-off distance, the implementation of cooling schemes, fuel/air ratio, etc. Experimental efforts in rig characterization will ultimately provide a better understand of the operating envelope and overall rig capabilities.

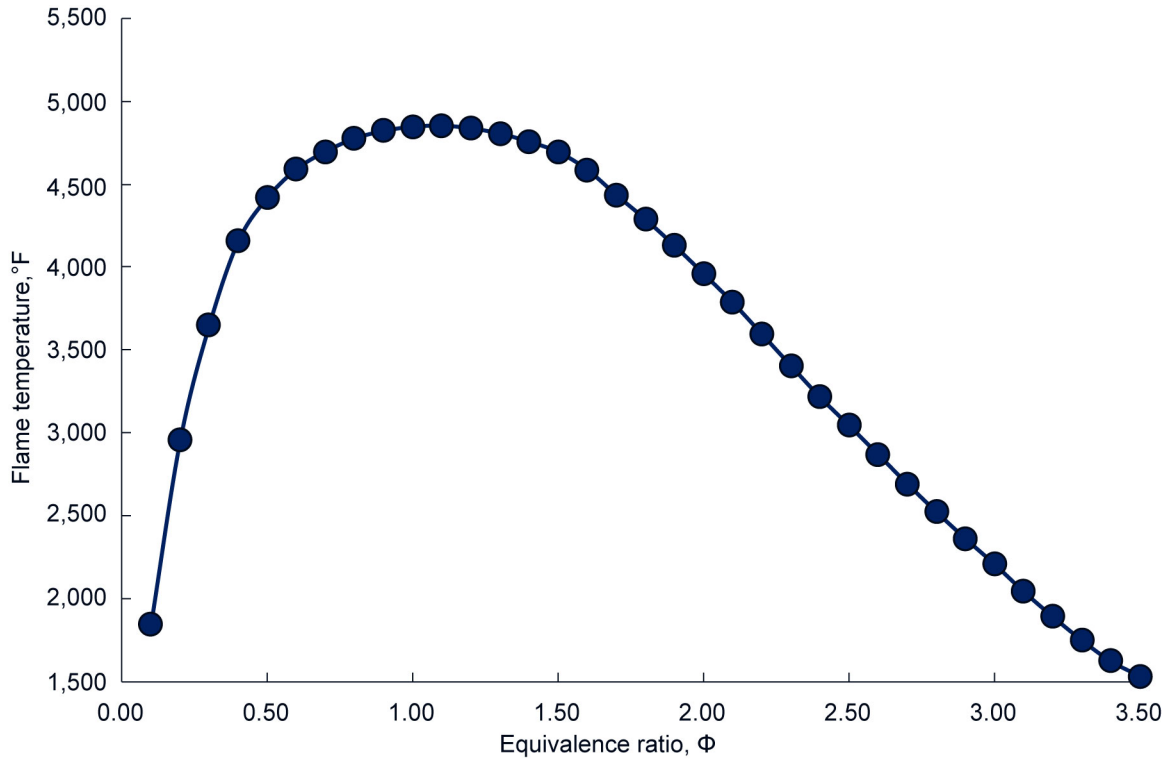

Figure 9.—Expected Flame Temperature (EFT) vs. Equivalence Ratio, Φ, calculated with CEA program for Natural Gas with 93 percent Oxygen (O_2) and 7 percent Nitrogen (N_2).

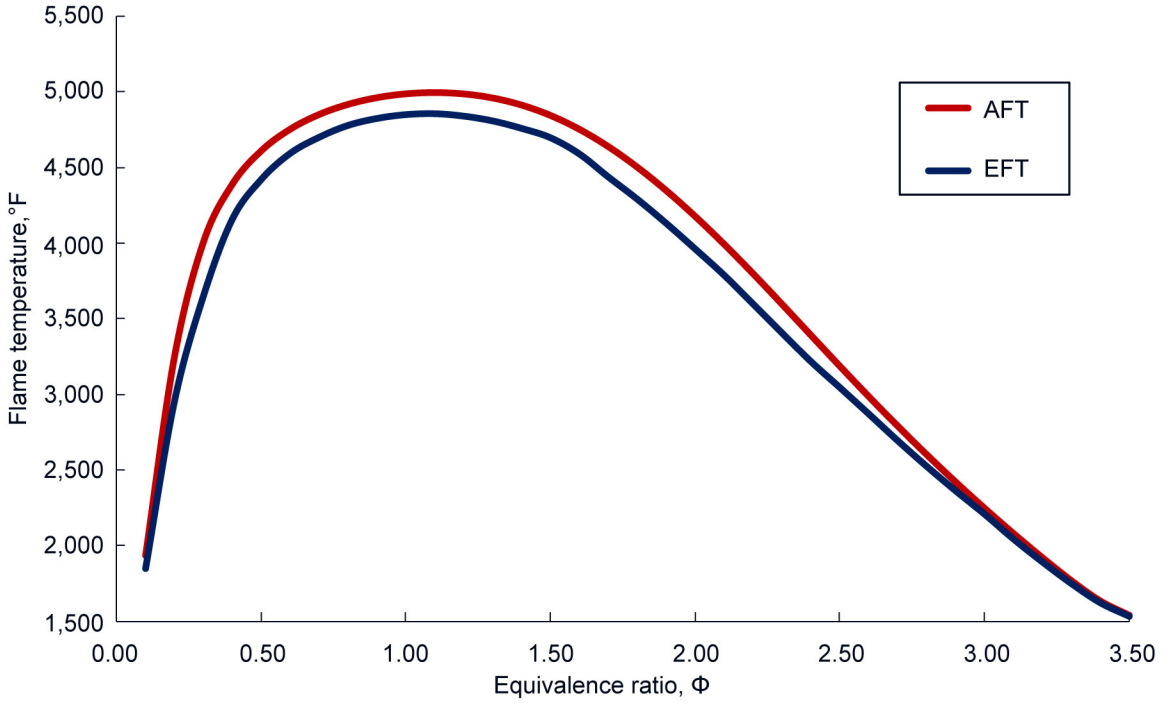

Figure 10.—Comparison of Adiabatic Flame Temperature (AFT) compared to Expected Flame Temperature (EFT) as a function of Equivalence Ratio, Φ calculated with the CEA program for Natural Gas with 93 percent Oxygen (O_2) and 7 percent Nitrogen (N_2).

TABLE II.—SUMMARY OF COMBUSTION ANALYSIS

NG/O_2 Burner Rig	Specification
Natural gas flow	31.7 lb/h (700 SCF/H)
Oxygen Enriched Air Flow, 93% by vol. O_2, 7% N_2	125.5 lb/h (1,500 SCF/H)
Heat released	639,100 BTU/h (187.1 kW)
AFT and EFT estimate at $\Phi = 1.0$	AFT = 4986 °F EFT = 4845 °F
Flame velocity	361 ft/sec (110 m/sec)
Heat flux estimate	~123 to 247 BTU/ft^2 (~140 to 280 W/cm^2)
Estimated sample temperature	From 1340 to 3140 °F (1000 to 2000 K)

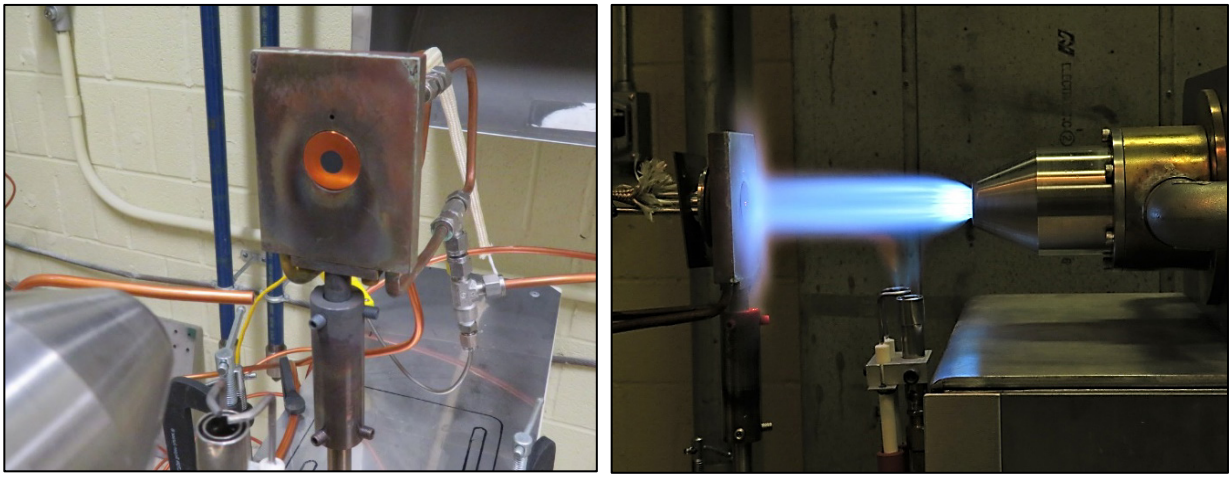

Figure 11.—Water-cooled, Gardon gauge heat flux sensor prior to and during exposure to the NG/O_2 flame.

4.0 Heat Flux Measurement

An initial measurement of heat flux was conducted with a MEDTHERM Corporation (Huntsville, AL) 64-Series Gardon Gauge water-cooled heat flux sensor (Figure 11). The sensor was positioned normal (90°) to flame at a 5.5 in. standoff distance from the front of the burner exit nozzle. Three heat flux curves were generated where the oxygen flow was held constant at 470 (minimum oxygen flow), 600, and 700 SCF/H while the natural gas flow was increased from a starting value of 25 SCF/H (the minimum flow used for ignition). The results are shown in Figure 12. Note that the fuel/air ratio in Figure 12 is by volume to correspond with the volumetric flow control of natural gas and oxygen using the PLC touchscreen. The measured heat flux increases with increasing fuel/air ratio until it reaches a maximum, which appears to occur for slightly rich mixtures, and then begins to decrease as the fuel/air ratio is increased further. The peak heat flux also appears to increase slightly with increasing flows. The measured heat flux ranged from approximately 30 to 210 W/cm^2 while the combustion analysis (Table II) estimated a heat flux of ~140 to 280 W/cm^2. However, care must be taken in interpreting the measured heat flux curves in Figure 12. The Gardon Gauge sensor is actively cooled using water, so the results in Figure 12 represent a cold-wall heat flux. In addition, the NG/O_2 burner rig environment is mixed mode,

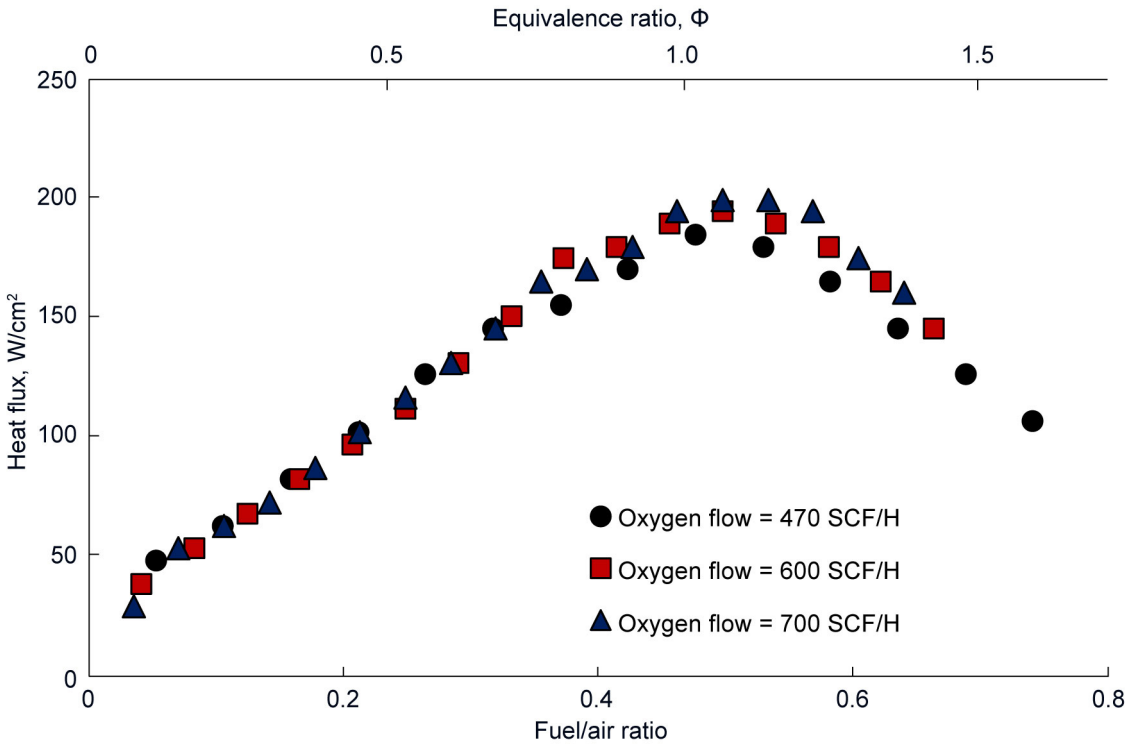

Figure 12.—Results of the heat flux measurements.

consisting of convective and radiative heat transfer. While water-cooled sensors such as the Gardon Gauge can be successfully implemented in mixed mode environments, corrections may be required (Refs. 8 and 9). As such, further work is warranted to better quantify and understand the heat flux in the NG/O_2 burner rig environment, particularly in the case for a hot-wall heat flux measurement.

5.0 Initial Material Durability Experiments

5.1 Oxidation and Recession of Monolithic Silicon Carbide

Silicon carbide (SiC) is a ceramic generally resistant to higher temperatures than most metals and alloys. Due to its high purity and high density, the material is stable in long term applications in dry air or oxygen due to the formation of protective silica (SiO_2) on the surface which parabolically slows the oxidation process (Ref. 10). However, in the hot section of a gas turbine engine environment the uncoated material is exposed to a high water vapor partial pressure from the combustion of jet fuel. In such an environment both oxygen and water vapor react with the ceramic to form the surface SiO_2 layer. However, at the same time the silica reacts with the water vapor to form gaseous $Si(OH)_4$. The result of these two simultaneous reactions is material recession of the on the order of 10 mils in 1000 hours of engine operation (Refs. 11 to 14).

In this study, the oxidation and recession of a monolithic silicon carbide bar (Saint-Gobain Performance Ceramics & Refractories, Worcester, MA) was studied. Per the technical data sheet (Ref. 15), Hexoloy® SA SiC is produced by pressureless sintering of submicron alpha silicon carbide powder. The sintering process results in a self-bonded, fine grain (less than 10 μm) SiC product which is extremely hard, lightweight and low in porosity. The material can be formed into complex shapes with greater than 98 percent theoretical density. Hexoloy® SA SiC is highly resistant to corrosion, erosion, sliding wear, high temperature and

thermal shock. It has a low coefficient of thermal expansion. The single-phase composition of the material enables it to reliably perform in air at temperatures in excess of 3450 °F.

Combustion of the jet fuel in our facility's Mach 0.3 burner rigs results in ~10 percent H_2O. That low water vapor pressure would result in simple oxidation of a SiC sample, with little to no recession observed. In the NG/O_2 burner rig, it is estimated that the combustion of natural gas provides up to ~40 percent H_2O. In that case, a high temperature exposure of uncoated SiC should result in material recession. In this experiment, 6- by 1- by 0.25-in. bars of Hexoloy SA SiC were exposed to various temperatures in 5 h increments (Figure 13 and Figure 14). The test matrix for the Hexoloy SA SiC bars is shown in Table III. The test temperature was measured on the leading edge of the bar using an Ircon 2-color pyrometer, and a FLIR A6798sc thermal imaging camera was implemented to measure thermal gradients along the sample length and width.

Figure 15 is a graphical representation of the sample weight change [mg] versus exposure time [h]. The oxidation-recession behavior for the 2400 °F sample was characteristic of paralinear behavior with an initial interval of weight gain prior to reaching a linear weight loss rate. For the 2700 and 3000 °F samples, an initial interval of weight gain was not observed. Post-test images of the sides and leading edges are displayed in Figure 16 to Figure 18 where differing silica scale thicknesses can be observed.

To calculate rate constants, specific weight change (i.e., weight change per unit surface area [mg/cm^2]) should be used rather than simply using weight change [mg] as plotted in Figure 15. However, the SiC bars are not uniformly heated as shown by the thermal profiles in Figure 19. As such, the competing mechanisms of oxidation and recession are occurring at different rates along the sample. Therefore, further work is warranted to understand the observed kinetics of the SiC bars in the NG/O_2 environment.

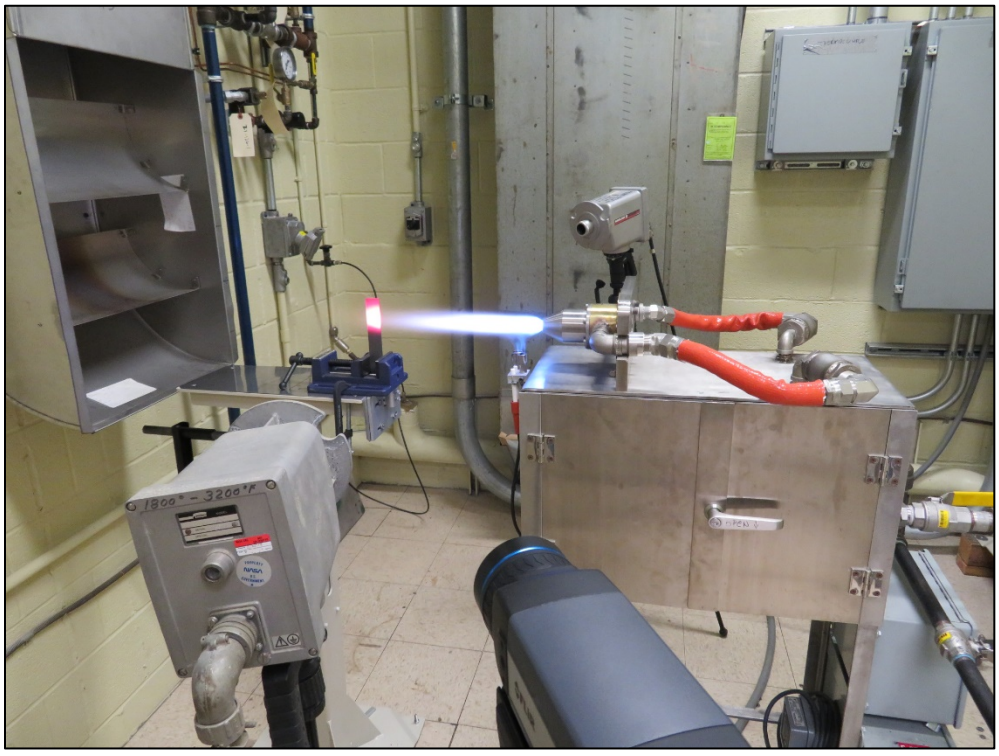

Figure 13.—Monolithic silicon carbide in test.

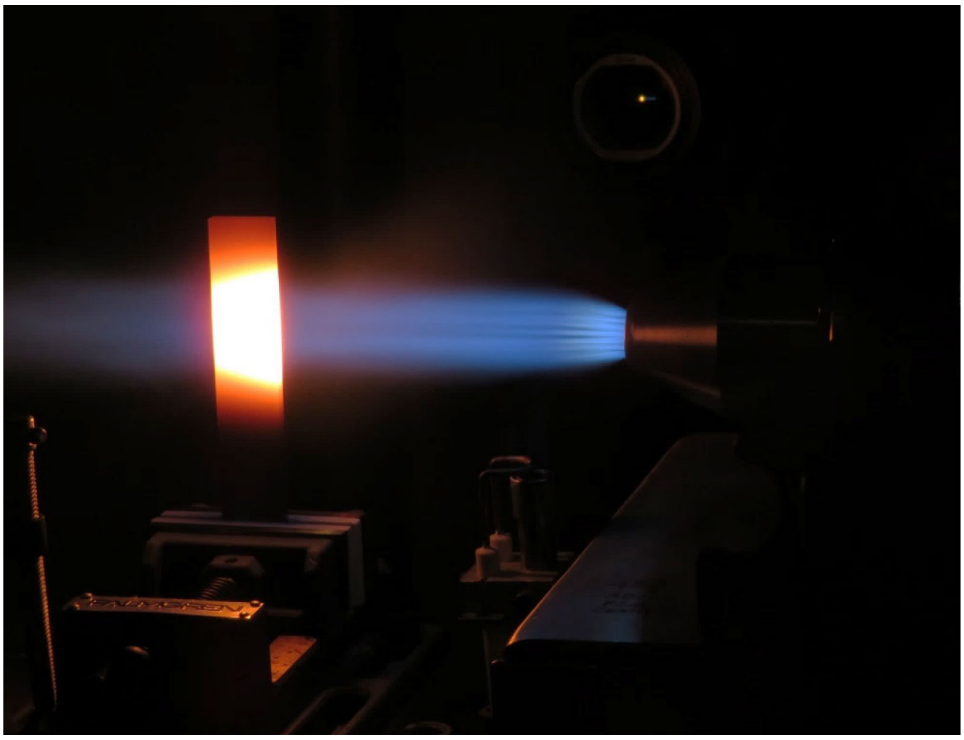

Figure 14.—Monolithic silicon carbide at 3,000 °F in test. Note temperature distribution. The “warm” top edge of the sample is clearly delineated. Sample is 1-in. wide.

TABLE III.—TEST MATRIX FOR SiC OXIDATION-RECESSION

Sample	Test temperature, °F	Natural gas, SCF/H	Oxygen, SCF/H
1	2400	84	470
2	2700	114	470
3	3000	165	470

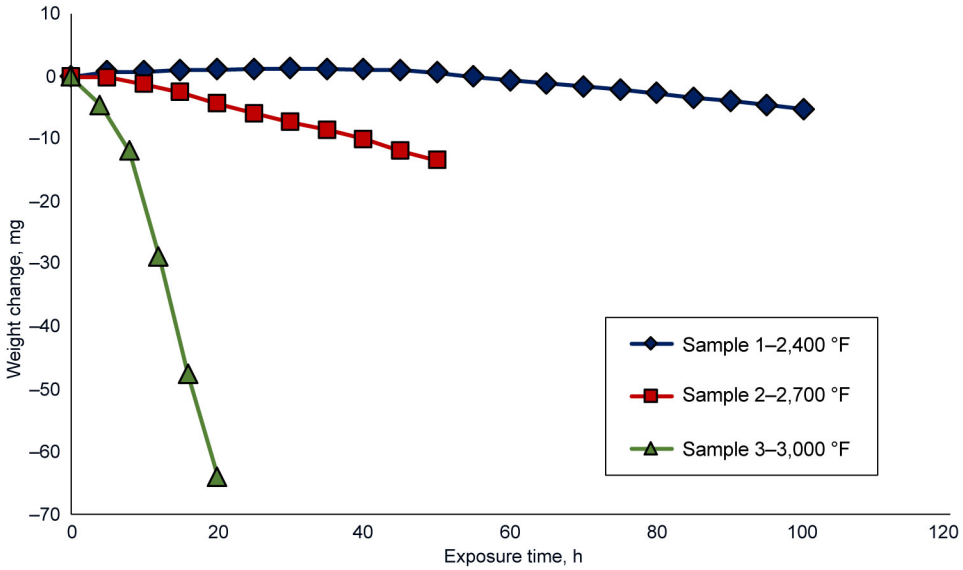

Figure 15.—SiC sample weight change vs. exposure time for the test conditions in Table III.

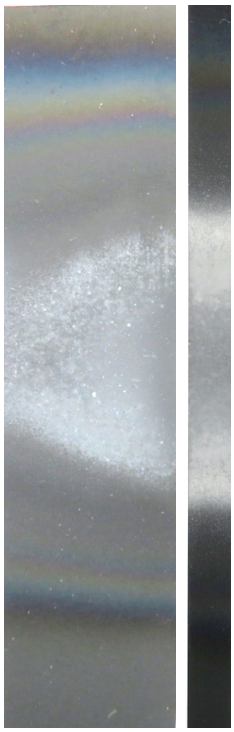

Figure 16.—Side view (1-in. width) and leading-edge view (0.25-in. width) of oxidized SiC after 100 h exposure at 2400 °F. Flame direction right to left.

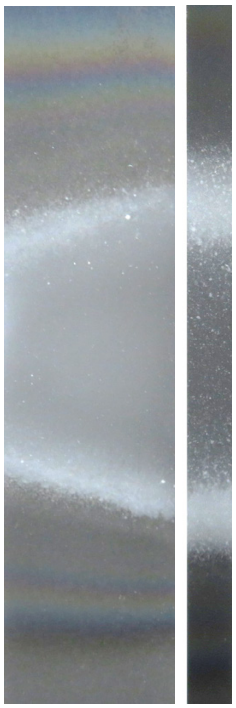

Figure 17.—Side view (1-in. width) and leading-edge view (0.25-in. width) of oxidized SiC after 50 h exposure at 2700 °F. Flame direction right to left.

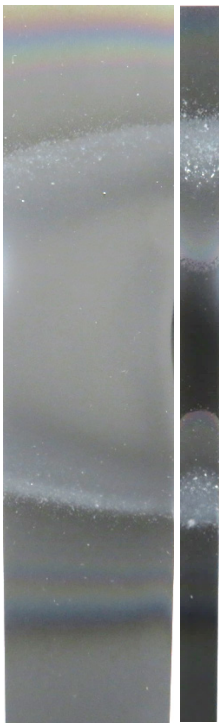

Figure 18.—Side view (1-in. width) and leading-edge view (0.25-in. width) of oxidized SiC after 20 h exposure at 3000 °F. Flame direction right to left.

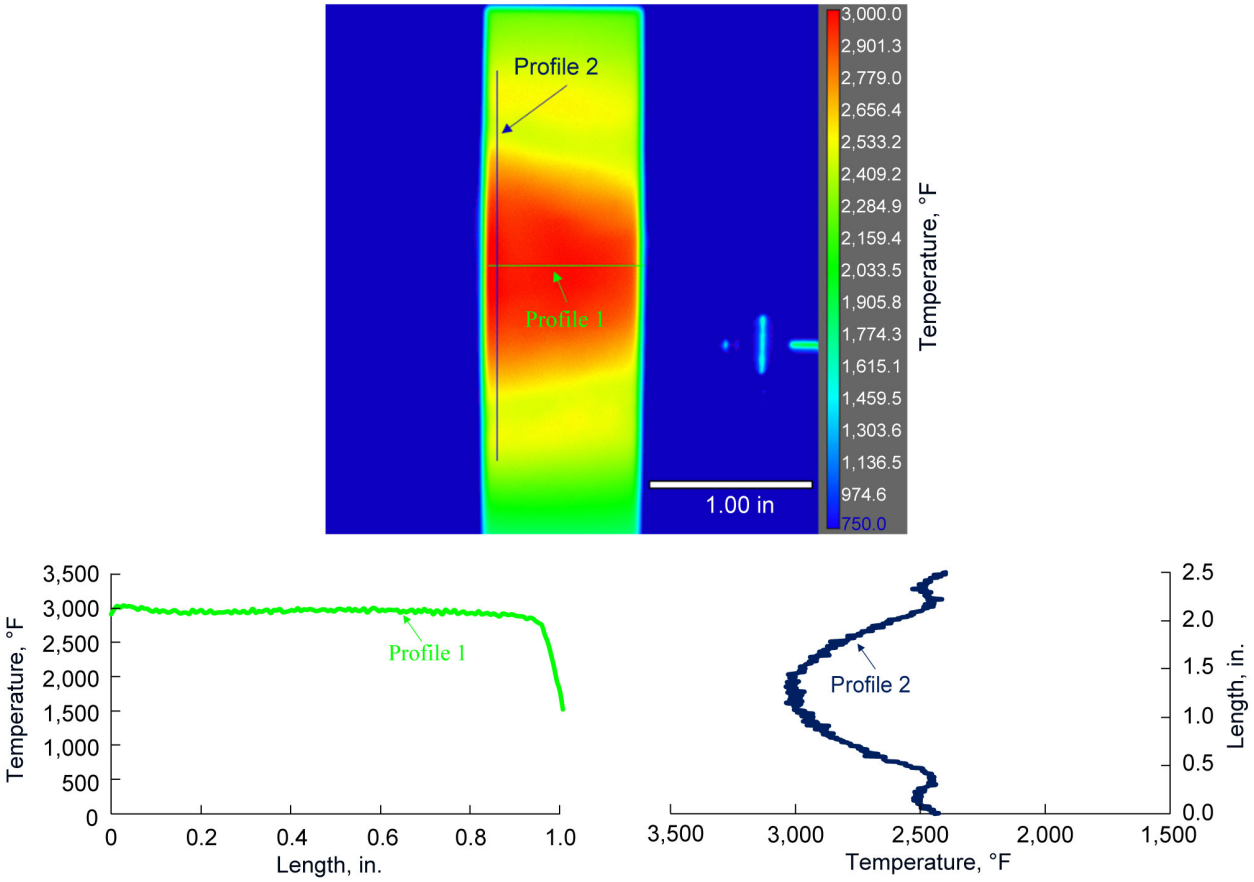

Figure 19.—FLIR thermal profile at 3000 °F showing thermal gradient. Flame direction left to right.

5.2 Ceramic Matrix Composite With Protective Environmental Barrier Coating

The development of high temperature structural ceramics for advanced gas turbine engines has been an area of active research for many years. This includes silicon carbide fiber reinforced silicon carbide matrix (SiC/SiC) composites. As noted in section 5.1, in such an application this material is exposed not only to high temperatures but also aggressive gases including water vapor. The result is oxidation to form SiO_2 and of its reaction with water vapor to form $Si(OH)_4$ that results in material recession. A class of protective materials known as environmental barrier coatings (EBCs) was developed to combat this problem (Ref. 16).

In this initial study, the durability of a flat 3- by 3-in. melt-infiltrated (MI) SiC/SiC ceramic matrix composite (CMC) panel was studied. The front side to be exposed to the NG/O_2 flame was coated with the 2400 °F capable NASA Generation II $Yb_2Si_2O_7$ EBC (Refs. 17 and 18). It should be noted that the 2400 °F denotes the upper temperature limit at the EBC/CMC interface. The opposite (or back) side was uncoated with the bare CMC exposed to ambient air. The sample was held at a 45° angle-of-attack with respect to flame. Burner nozzle to sample center “stand-off” distance was 6.75 in. A number of available noncontact temperature measurement instruments were used to monitor the EBC surface temperature and CMC backside temperature in this test as shown in Figure 20 and Figure 21. EBC surface temperatures of 2500, 2600, and 2700 °F were obtained using 470 SCF/H oxygen flow with 84, 105, and 114 SCF/H natural gas flow, respectively. Future efforts will focus on the durability of higher temperature capable EBC/CMC systems (e.g., 2700 °F capable CMC, as well as >3000 °F EBC).

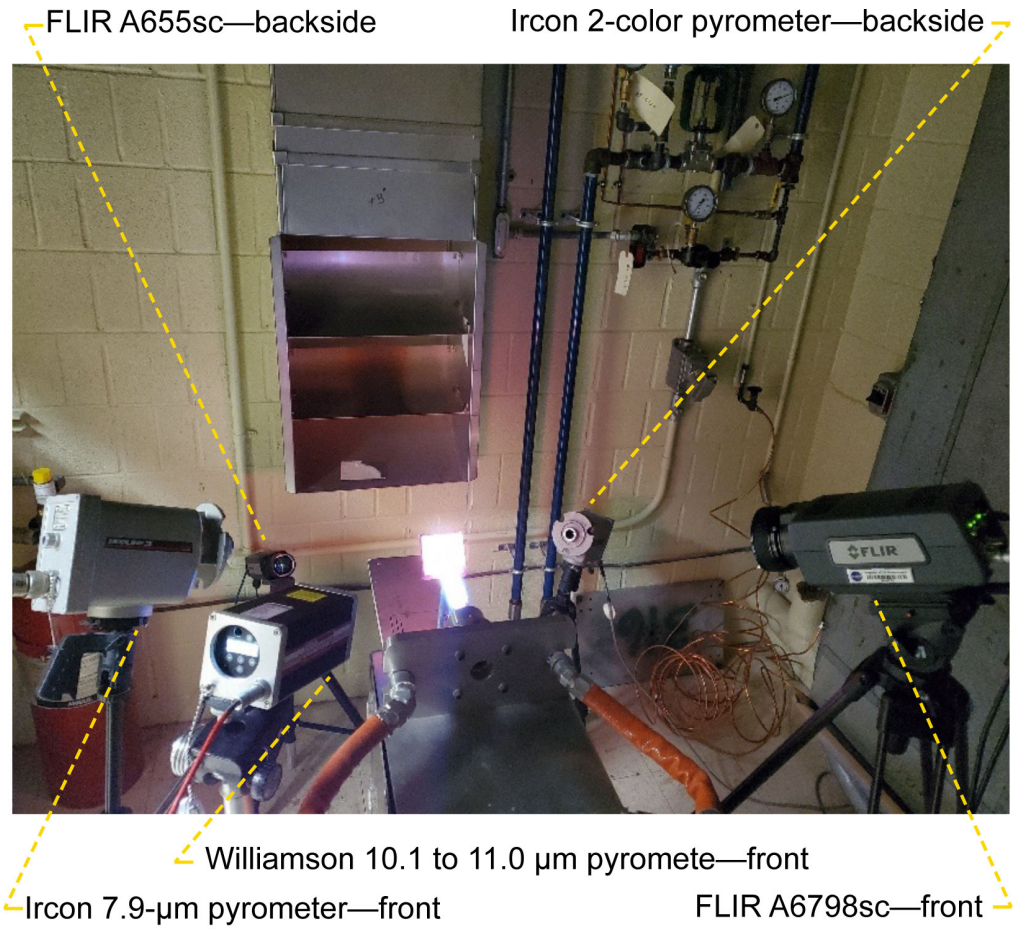

Figure 20.—Noncontact temperature measurement devices.

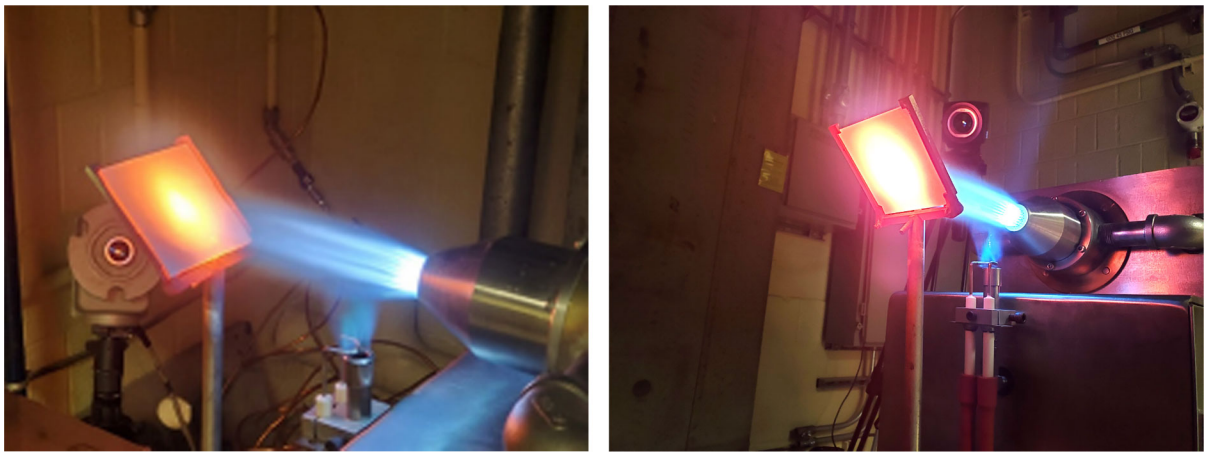

Figure 21.—The 3- by 3-in. CMC with front face EBC in test. Note dual electrode pilot burner to ignite and sense flame.

6.0 Summary

The focus of this Technical Memorandum was to present an overview of the natural gas/oxygen burner rig housed within the state-of-the-art NASA Glenn Burner Rig Facility. It is an atmospheric rig for testing in high heat flux oxidation environments to evaluate combined thermal-mechanical-environmental failure modes. The cost-effective rig is used as an efficient means of subjecting advanced

aircraft engine/exhaust materials to high temperatures and high velocities that closely approximate actual operating environments. Ceramic and metallic materials in various geometries and compositions are to be evaluated at temperatures up to and possibly greater than 3000 °F. These configurations include coupons, airfoils and leading edge geometries. Some tests are to be conducted on bare materials, but the rig will also be used to study the behavior and durability of protective coatings applied to each material class. These include environmental barrier coatings on Si-based ceramics and thermal barrier coatings on superalloys. Future improvements include providing active cooling, as well as implementing a static load frame for in-situ high temperature mechanical testing. The rig is primarily used to support NASA Aeronautics Research Mission Directorate (ARMD) programs.

References

1. D.S. Fox, R.A. Miller, D. Zhu, M. Perez, M.D. Cuy and R.C. Robinson "Mach 0.3 Burner Rig Facility at the NASA Glenn Materials Research Laboratory," NASA/TM—2011-216986.
2. http://carlislemachine.com/as_latheburners/grburner.php
3. https://ph.parker.com/us/en/polestar-smart-energy-saving-refrigerated-air-dryer-drd-series/drd250-230360-pa
4. https://www.ogsi.com/product/oxygen-generators/
5. https://www.ogsi.com/pressure-swing-adsorption-technology/
6. C.E. Baukal, Jr., *The John Zink Hamworthy Combustion Handbook.* CRC Press, Boca Raton, FL (2013).
7. B.J. McBride and S. Gordon, "Computer Program for Calculation of Complex Chemical Equilibrium Compositions and Applications, II: User's Manual and Program Description," NASA RP–1311 (1996).
8. Clayton A. Pullins and Tom E. Diller, "Direct Measurement of Hot-Wall Heat Flux," *Journal of Thermophysics and Heat Transfer*, 26 [3] 430–438 (2012). DOI: 10.2514/1.T3772.
9. Cecilia S. Lam, and Elizabeth J. Weckman, "Steady-State Heat Flux Measurements in Radiative and Mixed Radiative – Convective Environments," *Fire and Materials*, 33 [7] 303–321 (2009). DOI: 10.1002/fam.992.
10. J.A. Costello and R.E. Tressler, "Oxidation Kinetics of Hot-Pressed and Sintered α-SiC," *J. Am. Ceram. Soc*., 64 [6] 327–331 (1981).
11. E.J. Opila and R. Hann, "Paralinear Oxidation of CVD SiC in Water Vapor," *J. Am. Ceram. Soc*., 80 [1] 197–205 (1997).
12. E.J. Opila, D.S. Fox, and N.S. Jacobson, "Mass Spectrometric Identification of Si–O–H(g) Species from the Reaction of Silica with Water Vapor at Atmospheric Pressure," *J. Am. Ceram. Soc*., 80 [4] 1009–1012 (1997).
13. R.C. Robinson and J.L. Smialek, "SiC Recession Caused by SiO_2 Scale Volatility under Combustion Conditions: I, Experimental Results and Empirical Model," *J. Am. Ceram. Soc*., 82 [7] 1817–1825 (1999).
14. E.J. Opila, J.L. Smialek, R.C. Robinson, D.S. Fox, and N.S. Jacobson," SiC Recession Caused by SiO_2 Scale Volatility under Combustion Conditions: II, Thermodynamics and Gaseous-Diffusion Model," *J. Am. Ceram. Soc*., 82 [7] 1826–1834 (1999).
15. https://www.ceramicsrefractories.saint-gobain.com/sites/imdf.hpr.com/files/hexoloy-sa-sic-tds_0.pdf
16. K.N. Lee, D.S. Fox, and N.P. Bansal, "Rare Earth Silicate Environmental Barrier Coatings for SiC/SiC Composites and Si_3N_4 Ceramics," *J. Eur. Ceram. Soc*., 25 [10] 1705–1715 (2005).
17. K.N. Lee, "$Yb_2Si_2O_7$ Environmental Barrier Coatings with Reduced Bond Coat Oxidation Rates via Chemical Modifications for Long Life," *J. Am. Ceram. Soc*., 102 [3] 1507–1521 (2019).
18. K.N. Lee, A. Garg, and D. Jennings, "Effects of The Chemistry of Coating and Substrate on the Steam Oxidation Kinetics of Environmental Barrier Coatings for Ceramic Matrix Composites," *J. Eur. Ceram. Soc.,* 41 [11] 5675–5685 (2021).